Supporting Information

Monitoring supported lipid bilayers with n-type organic electrochemical transistors

Malak Kawan,[a] Tania C. Hidalgo,[a] Weiyuan Du,[b] Anna-Maria Pappa,[c] Róisín M. Owens,[c] Iain McCulloch,[b,d] Sahika Inal [a*]

[a] King Abdullah University of Science and Technology (KAUST), Division of Biological and Environmental Sciences and Engineering, Organic Bioelectronics Laboratory, Saudi Arabia.

[b] KAUST, KAUST Solar Center, Division of Physical Sciences and Engineering, Saudi Arabia.

[c] University of Cambridge, Department of Chemical Engineering and Biotechnology, UK.

[d] Imperial College London, Department of Chemistry and Centre for Plastic Electronics, UK

*sahika.inal@kaust.edu.sa

p(NDI-T2-L2) synthesis:

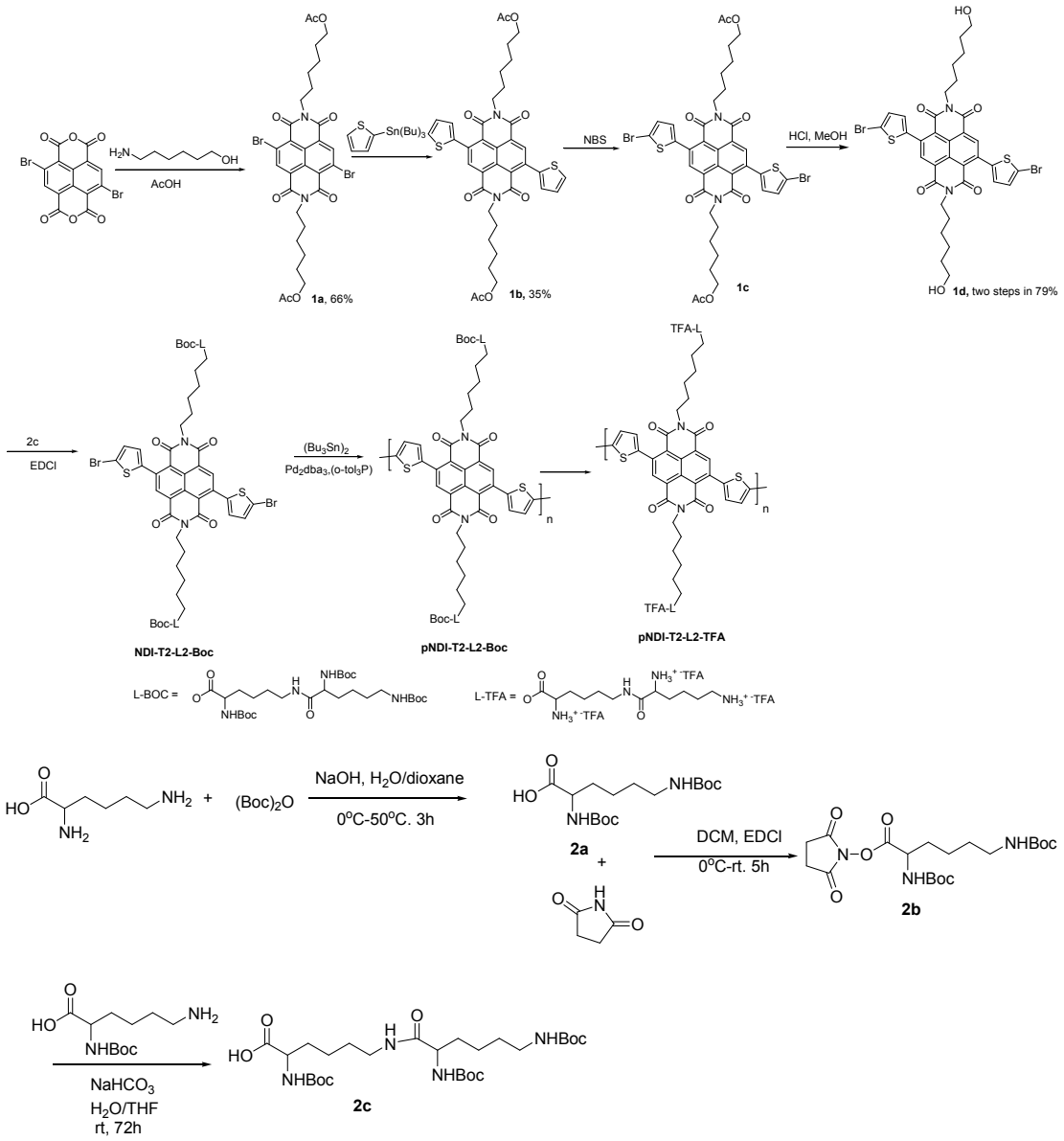

(4,9-dibromo-1,3,6,8-tetraoxo-1,3,6,8-tetrahydrobenzo[*lmn*][3,8]phenanthroline-2,7-diyl)bis(hexane-6,1-diyl) diacetate (1a). 4,9-Dibromoisochromeno[6,5,4-*def*]isochromene-1,3,6,8-tetraone (NDA-Br2) (4.26 g, 10 mmol) and 6-aminohexan-1-ol (3.51 g, 30 mmol) were added in acetic acid (100 mL). The reaction mixture was refluxed under Argon for 2 h. Then the reaction mixture was poured onto water and the resulting precipitate was filtered and washed with methanol. The crude product was used for next steps without further purification. **1a** was obtained

as a red-orange solid. Yield: 66 % (4.7 g). ^{1}H NMR (400MHz, DMSO, δ): 8.68 (s, 2H), 4.03-4.01 (m, 8H), 1.99 (s, 3H), 1.91 (s, 3H), 1.64-1.56 (m, 8H), 1.38-1.36 (m, 8H).

(1,3,6,8-tetraoxo-4,9-di(thiophen-2-yl)-1,3,6,8-tetrahydrobenzo[*lmn*][3,8]

phenanthroline-2,7-diyl)bis(hexane-6,1-diyl) diacetate (1b). After removing the air present by means of vacuum/nitrogen cycles, **1a** (4.7g, 6.6 mmol), tributyl(thiophen-2-yl)stannane (4.6 mL, 14.5 mmol), tris(dibenzylideneacetone)dipalladium(0) (5%, 300 mg) and tri(o-tolyl) (20 %, 401 mg) were added which thus degassed in 80 mL chlorobenzene for 15 mins. The temperature was then raised up to 100°C. After 5 hours at this temperature, chlorobenzene was removed under pressure and the crude was purified by silica gel chromatographic column with the elution (eluent: DCM/PE = 1/1 to 3/1). **1b** was obtained as red solid. Yield: 1.66 g (35%).

^{1}H NMR (400MHz, $CDCl_3$, δ): 8.75 (s, 2H), 7.58-7.57 (m, 2H), 7.30-7.29 (m, 2H), 7.22-7.20 (m, 2H), 4.11 (t, 4H), 4.03 (t, 4H), 2.03 (s, 6H), 1.71-1.68 (m, 4H), 1.63-1.59 (m, 4H), 1.41-1.39 (m, 8H); ^{13}C NMR (175 MHz, CDCl3, δ): 171.34, 162.31, 162.10, 140.78, 140.51, 136.83, 128.6, 128.12, 127.62, 127.58, 125.52, 123.61, 64.55, 41.11, 28.62, 28.00, 26.80, 25.79, 21.15.

(4,9-bis(5-bromothiophen-2-yl)-1,3,6,8-tetraoxo-1,3,6,8-tetrahydrobenzo[*lmn*][3,8]

phenanthroline-2,7-diyl)bis(hexane-6,1-diyl) diacetate (1c). 1b (1.42g, 2 mmol) was dissolved in mixture of $CHCl_3$/DMF at the ratio 2/1. NBS (0.747g, 4.2 mmol) was added to solution. And this mixture kept at 40 °C and was analyzed with NMR. After 3 hours, the reaction was completed and concentrated under vacuum. Then, methanol was added and resulting precipitate was filtered and washed with methanol. **1c** was obtained as purple solid and used for next step without purification. ^{1}H NMR (400MHz, $CDCl_3$, δ): 8.71 (s, 2H), 7.16-7.15 (m, 2H), 7.08-7.07 (m, 2H), 4.13-4.03 (m, 8H), 2.03 (s, 6H), 1.71-1.60 (m, 8H), 1.42-1.40 (m, 8H); ^{13}C NMR (175 MHz, CDCl3, δ): 171.35, 162.06, 162.03, 142.10, 139.32, 136.62, 130.33, 128.97, 127.67, 125.74, 123.38, 115.57, 64.53, 41.19, 28.61, 27.99, 26.79, 25.77, 21.16.

4,9-bis(5-bromothiophen-2-yl)-2,7-bis(6-hydroxyhexyl)benzo[*lmn*][3,8]phenanthroline-1,3,6,8(2*H*,7*H*)-tetraone (1d). 1c dissolved in a mixture of 100 mL $CHCl_3$, 20 mL MeOH and 5 mL conc. HCl. The mixture was refluxed, tracking with TLC. When the reaction was completed, the mixture was concentrated under vacuum. Then, methanol was added and resulting precipitate was filtered and washed with methanol. **1d** was obtained as purple solid. Yield for two steps:79%,

1.24g. ^{1}H NMR (400MHz, $CDCl_3$, δ): 8.71 (s, 2H), 7.16-7.15 (m, 2H), 7.08-7.07 (m, 2H), 4.13 (t, 4H), 3.63 (t, 4H), 1.72-1.69 (m, 4H), 1.59-1.54 (m, 4H), 1.44-1.41 (m, 8H). ^{13}C NMR (175 MHz, CDCl3, δ): 162.10, 162.06, 142.12, 139.34, 1365.64, 130.35, 128.97, 127.68, 125.76, 123.40, 115.58, 62.96, 41.19, 32.73, 28.06, 26.89, 25.50.

***N*^{2},*N*^{6}-bis(*tert*-butoxycarbonyl)lysine (2a).** A mixture of lysine (7.3 g, 50 mmol), NaOH (2.04 g, 51 mmol) and 200 ml THF/H_2O (1:1) was stirred at 0 °C, and dissolved $(Boc)_2O$ (27.2 g, 125 mmol) in anhydrous THF, which was then added to the mixture. The mixture was heated at 50 °C for another 3h. The mixture was then cooled to room temperature, concentrated under reduced pressure, adjusted the pH to 3, and extracted with ethyl acetate for three times. The product was dried with $MgSO_4$, and the solvent was removed to afford the oily **2a** (15 g, 86%). The product was then used without further purification. ^{1}H NMR (400 MHz, DMSO-d_6) δ (ppm) 7.00-6.98 (m, 1H), 6.77-6.76 (m, 1H), 3.82-3.79 (m, 1H), 2.90-2.85 (m, 2H), 1.52-1.52 (m, 2H), 1.37-1.25 (m, 22H).

2,5-dioxopyrrolidin-1-yl *N*^{2},*N*^{6}-bis(*tert*-butoxycarbonyl)lysinate (2b). A mixture of **2a** (3.45 g, 10 mmol) and NHS (1.38g, 12 mmol) in anhydrous DCM were stirred at 0 °C under argon. EDCI(4.5g, 24 mmol) was then added to the mixture. The mixture was stirred at 0 °C for another 0.5 h and 5.5 h at room temperature. The organic phase was washed with water for three times, and one time with $NaHCO_3$ aqueous solution, dried with $MgSO_4$, and the solvent was removed under reduced pressure. The product was then recrystallized with EA/Hexane to give the **2b** (4g, 90%). ^{1}H NMR (400 MHz, DMSO-d_6) δ (ppm) 7.55-7.54 (m, 1H), 6.78-6.77 (m, 1H), 4.29-4.26 (m, 1H), 2.90-2.79 (m, 6H), 1.39-1.36 (m, 24H).

N^6-(N^2,N^6-bis(tert-butoxycarbonyl)lysyl)-N^2-(tert-butoxycarbonyl)lysine (2c). 2b (2.2 g, 5 mmol), (*tert*-butoxycarbonyl)lysine (1.4g, 5.5 mmol) and $NaHCO_3$ (0.473g, 5.5 mmol) were dissolved in 50 ml THF/H_2O, stirred at room temperature of 3 days, and concentrated under reduced pressure to remove all solvent. The crude product was used without further purification. ^{1}H NMR (400 MHz, DMSO-d_6) δ (ppm) 7.76-7.73 (m, 1H), 7.01-6.99 (m, 1H), 6.76-6.69 (m, 2H), 3.83-3.77(m, 2H), 3.04-3.01 (m, 2H), 2.98-2.84 (m, 2H), 1.69-1.36 (m, 39H).

Monomer NDI-T2-L_2-BOC. In an oven dried flask, **1d** (0.588 g, 0.75 mmol) was dissolved in 10 mL dry DCM. EDCI (0.591 g, 3 mmol) and DIPEA (0.8 mL, 5 mmol) were added to this solution, followed by a solution of **2c** (Lysine-Boc, 1.435g, 2.5 mmol) in DCM and DMAP (0.122 g, 1mmol). The reaction was stirred at room temperature for overnight in dark. The reaction mixture was washed with water for 3 times. After drying the organic layer with $MgSO_4$, it was concentrated under reduced pressure at 40 °C and chromatographed (silica gel, 5% MeOH in DCM) to give **NDI-T2-L_2-BOC** (813 mg, 47%) as a red solid. ^{1}H NMR (400MHz, $CDCl_3$, δ): 8.71 (s, 2H), 7.16-7.15 (m, 2H), 7.08-7.07 (m, 2H), 6.26 (m, 2H), 5.18-5.17 (m, 4H), 4.62 (m, 2H), 4.25-4.24 (m, 2H), 4.20-3.99 (m, 12H), 3.27-3.21 (m, 4H), 3.09 (t, 4H), 1.79-1.34 (m, 92H);^{13}C NMR (175 MHz, CDCl3, δ): 172.94, 172.32, 162.08, 162.04, 156.33, 156.00, 155.65, 142.11, 139.31, 136.62, 130.34, 128.99, 127.69, 125.75, 123.40, 115.52, 80.18, 79.99, 79.34, 65.36, 54.55, 53.51, 41.48, 41.15, 38.96, 36.20, 32.22, 32.04, 29.83, 29.19, 29.16, 28.59, 28.56, 28.51, 28.48, 27.96, 27.80, 26.76, 25.68, 22.80, 22.76, 22.64, 20.58, 19.57, 18.90, 14.46, 11.57. MALDI-TOF calculated for C88H128Br2N10O22S2, 1898.701; found, 1900.856.

pNDI-T2-L2-BOC. A mixture of monomer **NDI-T2-L2-BOC** (108 mg, 0.0567 mmol), 2,5-1,1,1,2,2,2-hexabutyldistannane (33 mg, 0.0567 mmol), $Pd_2(dba)_3$ (1.2 mg), P(o-tolyl)$_3$ (1.8 mg) and degassed DMF (4 mL) was vigorously stirred at 80 °C under argon for 24h. After cooling to room temperature, the mixture was poured into Et_2O and the precipitate was collected by filtration. The crude polymer was purified in Soxhlet apparatus, washed with n-hexane, and with acetone sequentially. The acetone fraction was concentrated and poured into Et_2O. The polymer was recovered by filtration and dried in vacuum overnight. Yield: (79 mg, 81 %).

pNDI-T2-L2-TFA. 5 mL trifluoroacetic acid was added into solution of **pNDI-T2- L2-TFA** (47 mg) in 30 mL $CHCl_3$. The mixture was concentrated after stirring 2h at room temperature, then poured into Et_2O and the precipitate was collected by filtration. The collection was dried after washing with $CHCl_3$ for three times to afford dark solid with the yield (34 mg, 72%).

pNDI-T2-$C_{8,12}$. A mixture of monomer **NDI-T2-$C_{8,12}$** (114.2 mg, 0.1mmol), 2,5- 1,1,1,2,2,2-hexabutyldistannane (33 mg, 0.1 mmol), $Pd_2(dba)_3$ (1.8 mg), P(o-tolyl)$_3$ (2.4 mg) and degassed toluene (5 mL) was vigorously stirred at 100 °C under argon for 24h. After cooling to room temperature, the mixture was poured into MeOH and the precipitate was collected by filtration. The crude polymer was purified in Soxhlet apparatus, washed with n-hexane, acetone and

chloroform sequentially. The chloroform fraction was concentrated and poured into MeOH. The polymer was recovered by filtration and dried in vacuum overnight. Yield: (72 mg, 73 %).

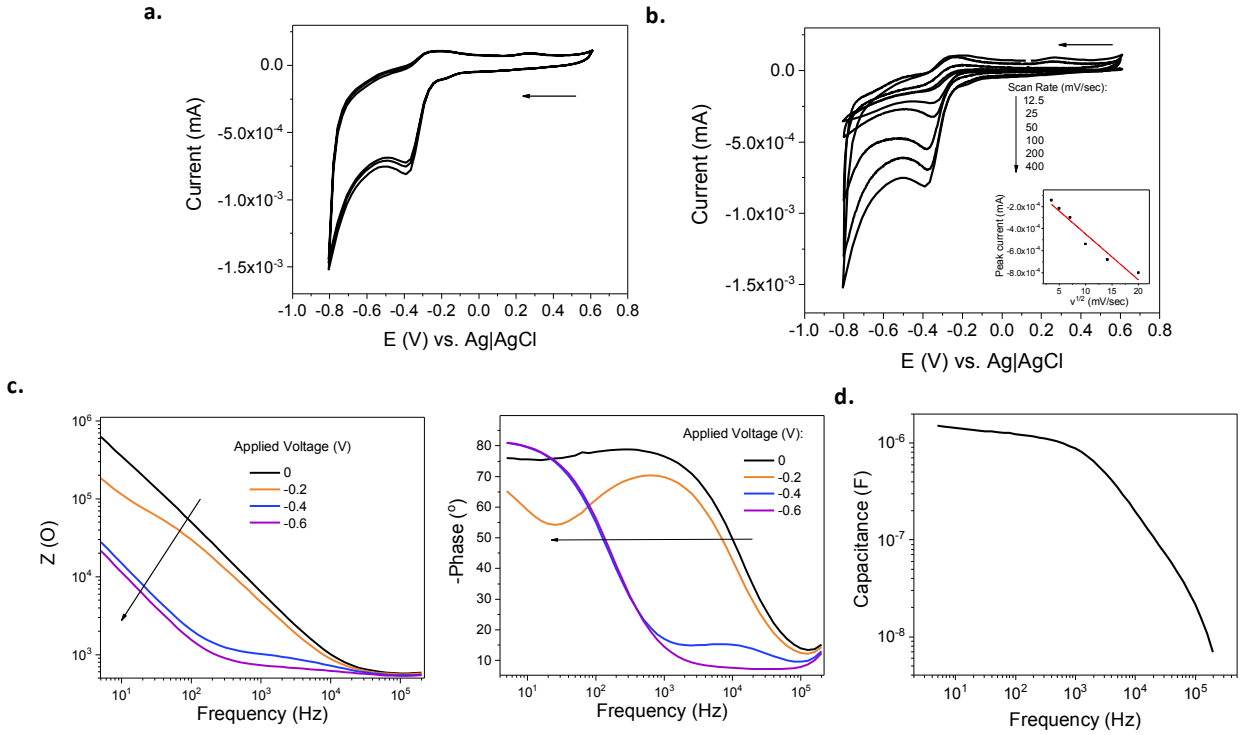

Figure S1. Electrochemical characterization of the n-type film. a. Cyclic voltammetry (CV) curve of the p(NDI-T2-L2) film measured in PBS. Three consecutive cycles are shown. **b.** CV curve of the p(NDI-T2-L2) film recorded with different scan rates (12.5, 25, 50, 100, 200, 400 mV/sec), inset: dependence of redox peak current on the square root of the scan rate. **c.** The magnitude of impedance and its phase recorded when the p(NDI-T2-L2) film was subject to different doping potentials (0, -0.2, -0.4, -0.6 V vs Ag/AgCl). **d.** Capacitance vs frequency plot extracted from the impedance characteristics measured at -0.6 V vs Ag/AgCl.

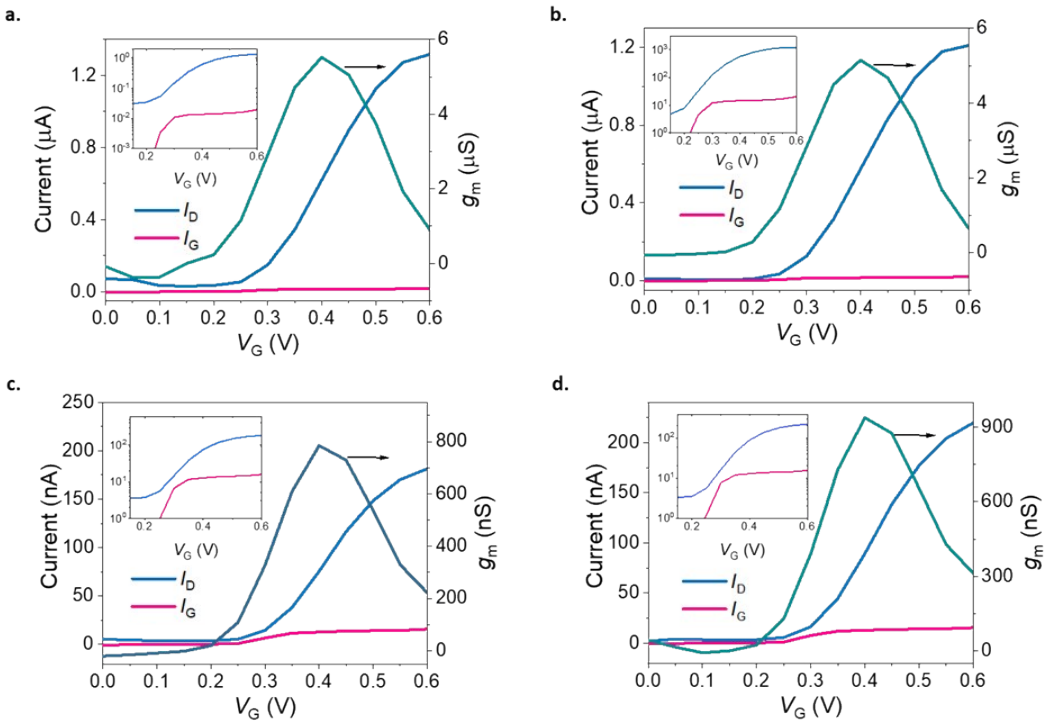

Figure S2. Transfer (I_D-V_G) curves recorded at V_D = 0.6 V along with the measured gate current, I_G, and the transconductance, g_m. g_m vs V_G curves refer to right axes. Curves are shown both on a linear scale, as well as on a logarithmic scale (inset). In **a.** and **b.** the devices have been pre-cycled in $CaCl_2$ whereas **c.** and **d.** are the typical devices. All devices were measured in 1X PBS with Ag/AgCl gate electrode.

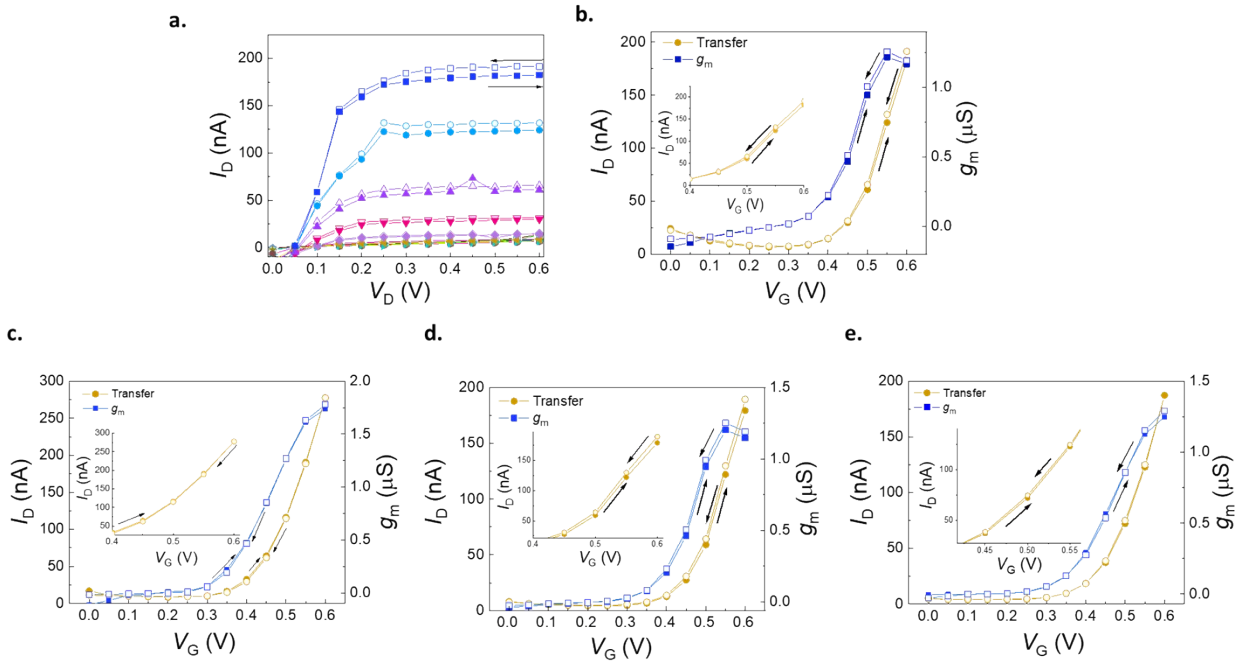

Figure S3. Hysteresis curves of p(NDI-T2-L2) OECTs. a. The output characteristics of the device for V_G increasing from 0 – 0.6 V in PBS. The arrows indicate the scan direction. **b-e.** Transfer curves of different channels along with transconductance values at V_D = 0.45 V where arrows indicate the direction of current hysteresis. inset: zoomed view of the forward and backward scans in the transfer curves. The scan rate is 2 V/s in all except in e) where it is 0.02 V/s. These experiments were performed seven months after the first fabrication and use of these devices in OECT experiments, and the devices have been left in ambient conditions.

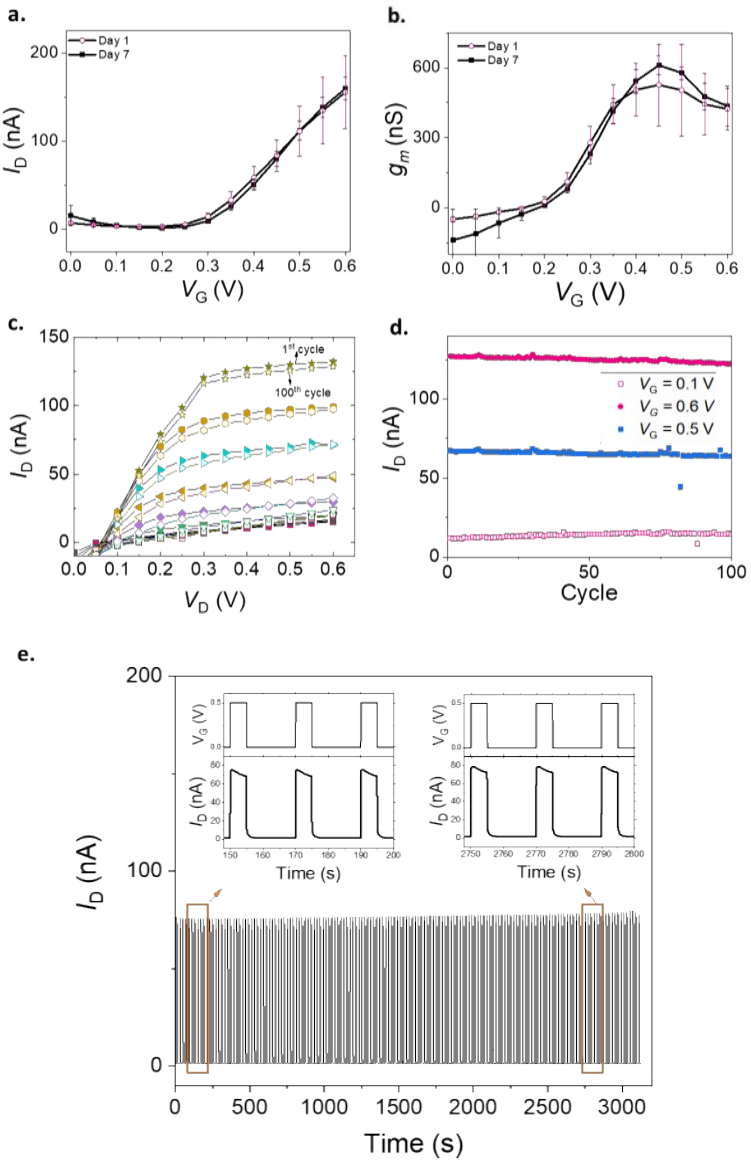

Figure S4. The stability of the n-type OECT. a. The drain current (I_D) and **b.** transconductance (g_m) of OECTs comprising p(NDI-T2-L2) in the channel *vs* gate voltage measured in day 1 and day 7. The devices have been used several times for similar measurements during this one week. The electrolyte is PBS, and V_D = 0.6 V. The error bars represent the standard deviation of the measured average derived from 3 different channels. **c.** Successive output curves of the n-type OECT with increasing V_G (0 – 0.6 V). First cycle (filled symbol) and 100th cycle (unfilled symbol) are indicated. **d.** Stability of the drain current at V_D = 0.4 V during 100 cycles at different gate biases (0.1, 0.5, and 0.6 V). **e.** Long-term pulsing of the p(NDI-T2-L2) OECT in PBS for 60 min (V_G = 0.5 V and V_D = 0.4 V) inset: a close-up comparing the drain current at the beginning and end

of the experiment. The experiments in **c-e** were performed with devices that have been used seven months after their first fabrication and excessive use in various other experiments. During this time, these devices have been stored in air.

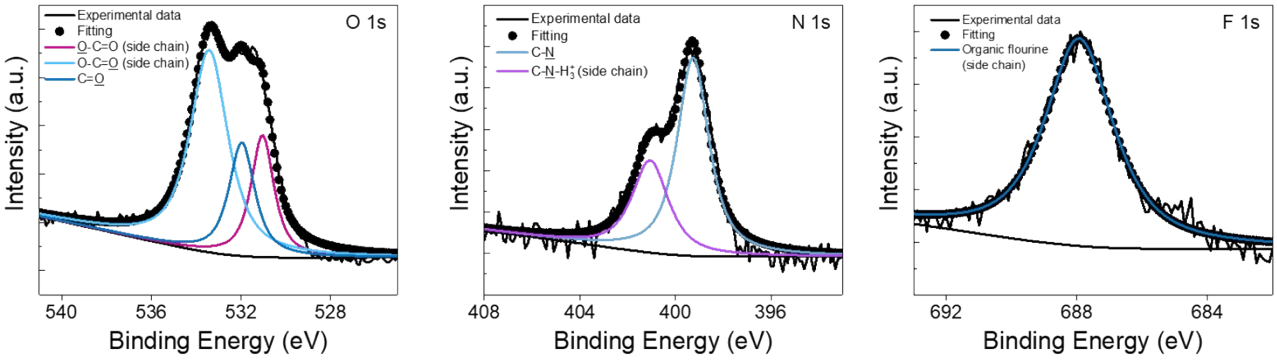

Figure S5. XPS analysis of the n-type film. High-resolution deconvoluted XPS spectra for O 1s, N 1s, and F 1s. The data were acquired using a step of 0.1 eV. The plots indicate the bonds that are present only in the side chain.

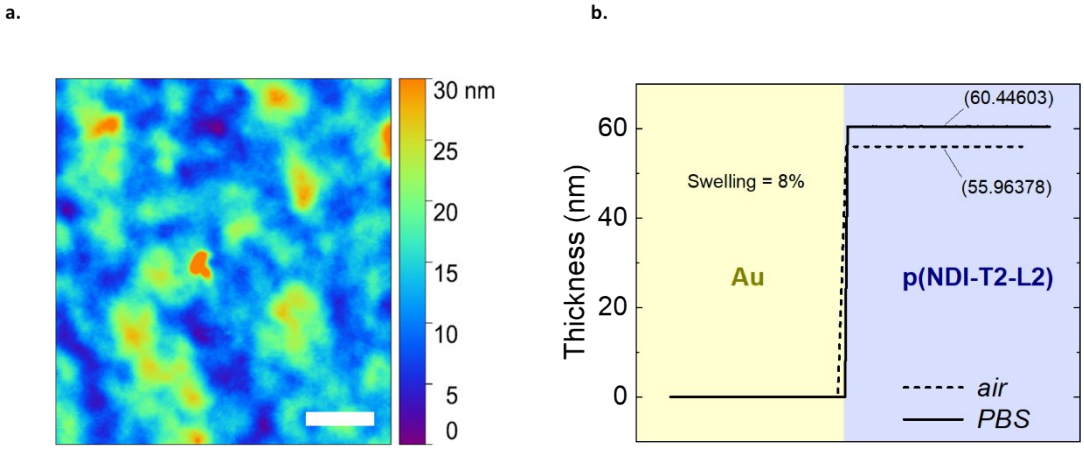

Figure S6. Surface roughness and swelling of a p(NDI-T2-L2) film. a. Atomic force microscopy (AFM) image (5 µm x 5 µm) of a p(NDI-T2-L2) film in air. Scale bar is 1 µm. **b.** QCM-D measurements showing the changes in the thickness of the p(NDI-T2-L2) film cast on Au

sensor as it was exposed to PBS. The initial film thickness is 56 nm and it becomes 60 nm upon swelling.

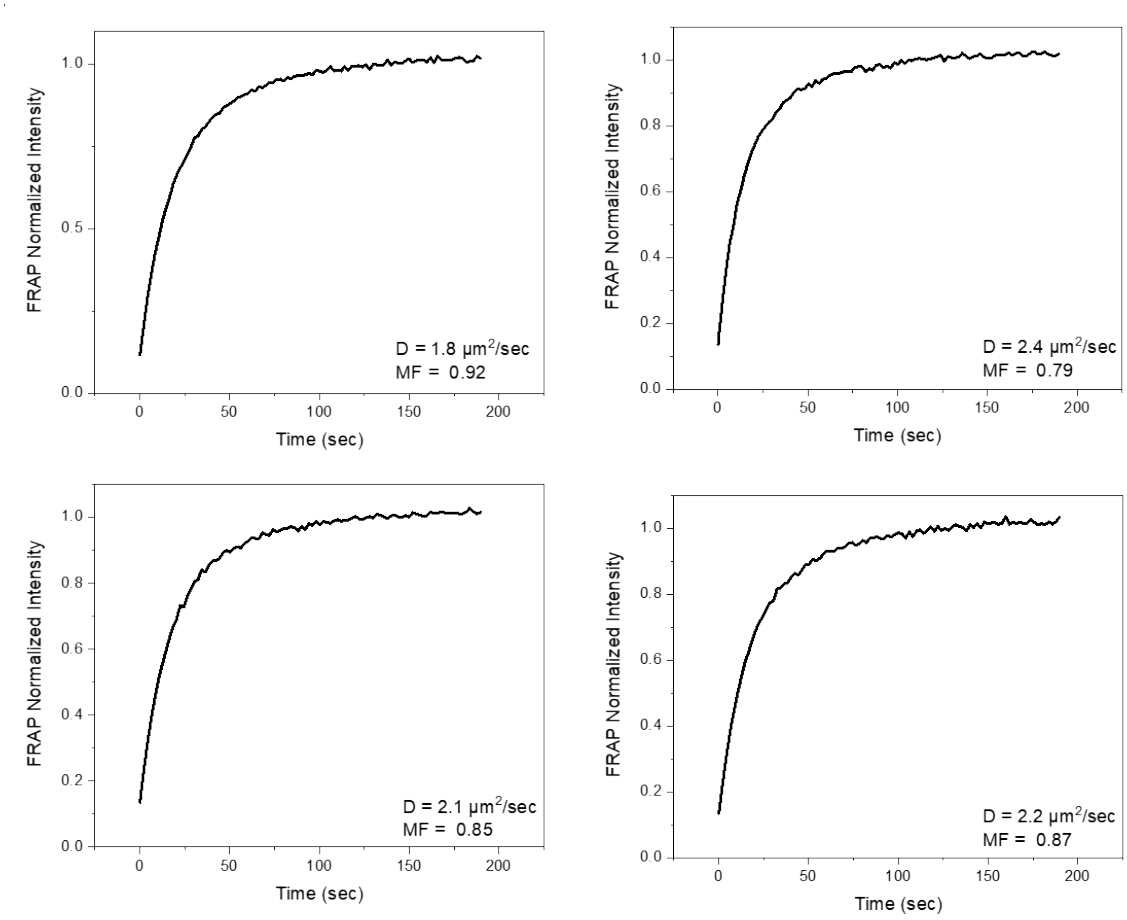

Figure S7. FRAP analysis experiments of SLB on p(NDI-T2-L2) films for Figure 2. Insets show mobile fraction (*MF*) and diffusion coefficient (*D*) of BODIPY-DHPE labeled DOPC bilayer. *MF* and *D* were calculated using ZEN 2009 software. Fluorescence intensity recovery is measured over time for four FRAP experiments.

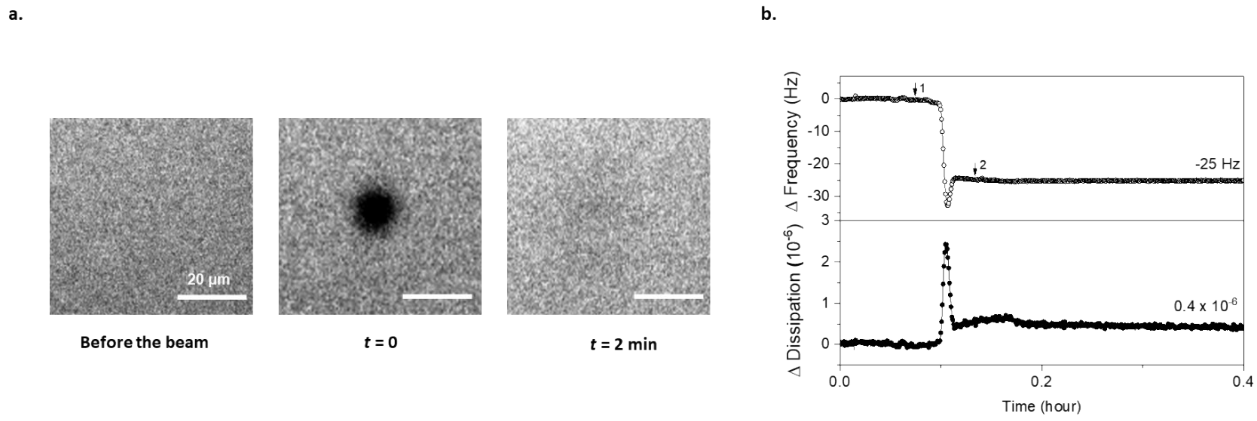

Figure S8. Characterizing DOPC on glass substrate via FRAP and QCM-D. a. FRAP images taken before the beam and after photobleaching at t = 0 and t = 2 min (from left to right). **b.** Frequency (hollow circles) and energy dissipation (filled circles) shift responses for DOPC lipid vesicles on silica-based sensor surface. Step 1: vesicle addition, Step 2: PBS rinse. The measurement values show the final frequency and energy dissipation shifts measured by the third harmonic.

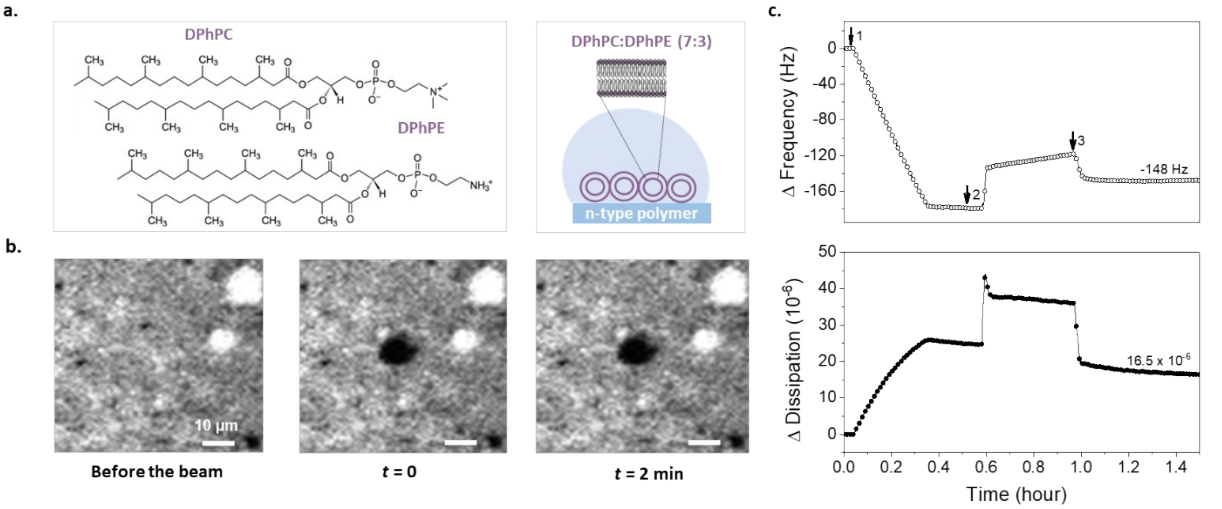

Figure S9. Characterizing non-fusing vesicles on p(NDI-T2-L2) films via FRAP and QCM-D. a. Chemical structure of DPhPC:DPhPE vesicles used to interface the polymer surface and a schematic depicting an assembly of lipid vesicles on the p(NDI-T2-L2) surface without fusion,

used as negative control. **b.** FRAP images taken before the beam and after photobleaching at t = 0 and t = 2 min (from left to right). **c.** Frequency (hollow circles) and energy dissipation (filled circles) shift responses for DPhPC:DPhPE lipid vesicles on p(NDI-T2-L2) coated sensor surface. Step 1: vesicle addition, Step 2: osmotic shock, Step 3: PBS rinse. The measurement values show the final frequency and energy dissipation shifts measured by the third harmonic.

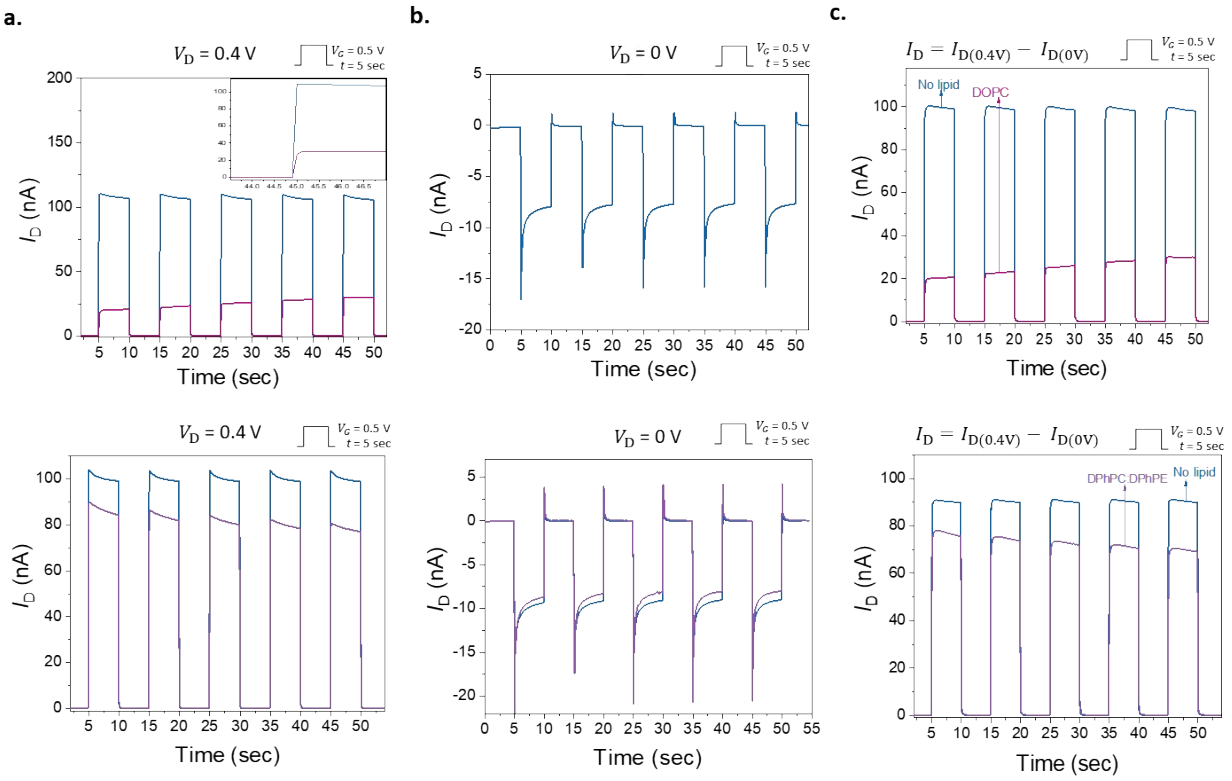

Figure S10. Transient characteristics of SLB integrated p(NDI-T2-L2) channels. a. Drain current (I_D) vs time before (blue) and after the addition of lipid vesicles: DOPC (pink; top), DPhPC:DPhPE (purple; bottom) (V_D = 0.4 V, V_G = 0.5 V). Inset: zoomed view (x axis: time; y axis: I_D). **b.** Capacitive current component shown before the addition of lipids (blue) and with DPhPC:DPhPE (purple; bottom) at V_D = 0 V (V_G = 0.5 V). **c.** Response time measurements after subtracting the capacitive current component of the SLB-free channel (blue) and after the addition of lipid vesicles: DOPC (pink; top), DPhPC:DPhPE (purple; bottom).

Here, a capacitive current component was detected in Figure S10a for the pristine device (lipid-free) and after the addition of DPhPC:DPhPE lipid vesicles. We subtracted the drain current measured at $V_D = 0$ V (Figure S10b) from the drain current at $V_D = 0.4$ V (Figure S10a), leading to the curves in Figure S10c.

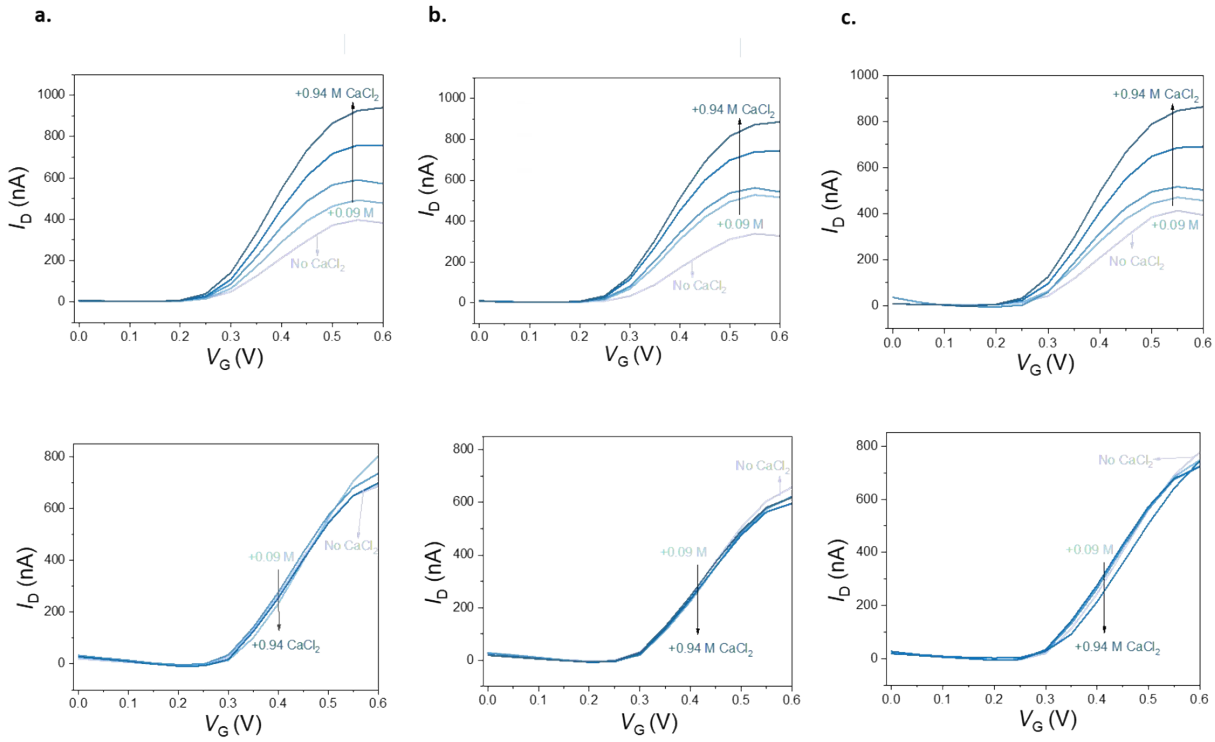

Figure S11. Ca^{+2} effect on the n-type channel with and without the DOPC lipid bilayer. Transfer curves of OECT channels before (top) and after the SLB formation (bottom) on p(NDI-T2-L2) in the presence of different concentrations of $CaCl_2$ (0.09 – 0.94 M, lightest to darkest blue, respectively). V_D= 0.6 V. "No $CaCl_2$" curve was measured in PBS. The titrations of $CaCl_2$ were done into PBS. **a.-c.** Transfer curves of different OECT channels.

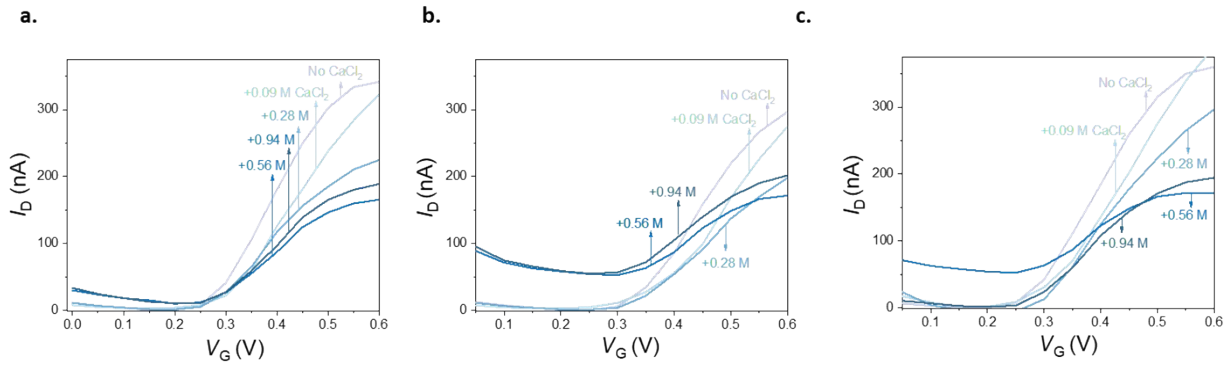

Figure S12. Blocking GA channels in DOPC lipid bilayer with Ca^{+2}. Transfer curves of p(NDI-T2-L2) based OECT channels after the formation of a DOPC bilayer with inbuilt GA (0.1 mg/mL) in the presence of different concentrations of $CaCl_2$ (0.09 – 0.94 M, lightest to darkest blue, respectively). V_D= 0.6 V. "No $CaCl_2$" curve was measured in PBS. The titrations of $CaCl_2$ were done into PBS. **a.-c.** Transfer curves of different OECT channels.

Table S1. The performance of p(NDI-T2-L2) OECTs gated in PBS. The product of electron mobility (μ) with volumetric capacitance (C*), i.e., μ × C* is calculated fro $m\, g_m = \frac{Wd}{L}\mu C^*(V_T - V_G)$. C* is determined using electrochemical impedance spectroscopy. The channel dimensions are 10 μm (length) × 100 μm (width), and the film thickness is ~100 nm. Best performing device performance is given along with the average ones.

OECT figures of merit

Peak current$_{max}$ (μA)	Peak current$_{avg}$ (μA)	g_{m_max} (μS)	g_{m_avg} (μS)	$(\mu \times C^*)_{max}$ ($Fcm^{-1}V^{-1}s^{-1}$)	$(\mu \times C^*)_{avg}$ ($Fcm^{-1}V^{-1}s^{-1}$)	V_T (V)	C* (Fcm^{-3})	ON/OFF
1.3	0.19±0.02	5.2	0.84± 0.09	0.31	0.046±0.004	0.22	95	ca. 220

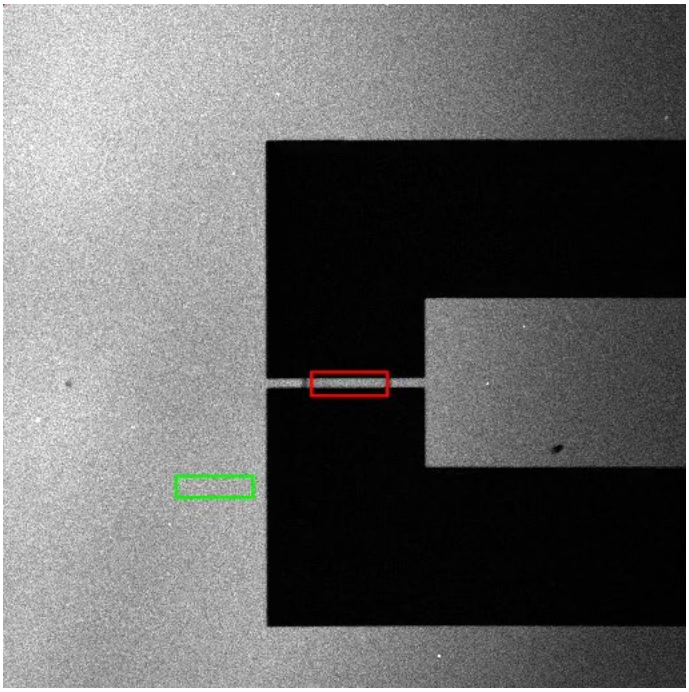

Video S1. FRAP experiment performed on the channel of an OECT.